

Size effect on the ferroelectric phase transition in $\text{SrBi}_2\text{Ta}_2\text{O}_9$ nanoparticles

T. Yu and Z. X. Shen^{a)}

Physics Department, National University of Singapore, 2 Science Drive 3, Singapore 117542, Singapore

W. S. Toh, J. M. Xue, and J. Wang

Materials Science Department, National University of Singapore, 2 Science Drive 3, Singapore 117542, Singapore

(Received 24 January 2003; accepted 28 April 2003)

We report the size effect on the ferroelectric phase transition in $\text{SrBi}_2\text{Ta}_2\text{O}_9$ nanoparticles. Samples with particle sizes between 11 and 71 nm were prepared by a room-temperature mechanical activation process followed by postannealing at different temperatures. The size of the particles was determined by x-ray diffraction with the aid of Scherrer's equation. The ferroelectric phase transition in both $\text{SrBi}_2\text{Ta}_2\text{O}_9$ nanoparticles and bulk sample were investigated by *in situ* Raman scattering. The results show that the transition temperature (T_c) decreases from its bulk value (605 K) as the size decreases. The size dependence of T_c can be described as $T_c = 605 - 1150/(D - 2.1)$ (K), where D (nm) is the particle size. A critical size of 2.6 nm, below which ferroelectricity disappears, was obtained from this empirical expression. © 2003 American Institute of Physics. [DOI: 10.1063/1.1583146]

I. INTRODUCTION

In recent years ferroelectric materials have attracted a lot of attention for use in nonvolatile memory devices, in particular, ferroelectric random access memories (FeRAM).¹⁻³ The leading candidate for this application is $\text{PbZr}_{1-x}\text{Ti}_x\text{O}_3$ (PZT) perovskite which has a high Curie temperature and large remanent polarization. However, PZT thin films exhibit serious polarization fatigue during electric field cycling. More recently, a significant breakthrough for controlling the fatigue problems was reported in which ferroelectric materials belonging to the layered perovskite family, such as $\text{SrBi}_2\text{Ta}_2\text{O}_9$ (SBT), show essentially no polarization fatigue with electric field cycling.⁴

$\text{SrBi}_2\text{Ta}_2\text{O}_9$ is a bismuth-layered pseudo-perovskite oxide. The crystal structure consists of $[\text{Bi}_2\text{O}_2]^{2+}$ layers and perovskite-type $[\text{SrTa}_2\text{O}_7]^{2-}$ units with double TaO_6 octahedral layers. Neutron and electron diffraction studies revealed that orthorhombic distortion with noncentrosymmetric space group $A2_1$ am is responsible for the displacive-type ferroelectric behavior.^{5,6} The atomic displacements along the a axis from corresponding positions in the paraelectric phase with a parent tetragonal ($I4mmm$) structure occur at the Curie temperature, $T_c = 608 \text{ K}$ ⁷ and these displacements cause the spontaneous ferroelectric polarization in SBT.

The effects of particle size on the physical properties of ferroelectric materials, especially the nanocomposites of electronic devices, have been extensively investigated theoretically using transverse the Ising model^{7,8} and Landau phenomenological theory^{9,10} and experimentally by x-ray diffraction (XRD)^{11,12} and Raman scattering.¹³ Frey *et al.*¹⁴ studied the effect of particle size on the crystal structure of BaTiO_3 ; Ishikawa, Yoshikawa, and Okada¹³ investigated the

effect of particle size on the Curie temperature in PbTiO_3 (PT); and the study in size effects on dielectric properties of $\text{PbZr}_{1-x}\text{Ti}_x\text{O}_3$ (PZT) was reported by Huang *et al.*¹⁰ In this article we present an *in situ* Raman scattering study of size effect on the ferroelectric phase transition in SBT ultrafine particles.

II. EXPERIMENT

The mechanical activation process has been described in detail in our previous studies.^{11,15} The starting materials used in this work were commercially available SrO (99.9% in purity, Sigma-Aldrich Chemical Company, Inc.), Bi_2O_3 (99.9% in purity, Acros Organics), and Ta_2O_5 (99% in purity, Sigma-Aldrich Chemical Company, Inc.) After 30 h mechanical activation of the starting mixed oxides, the as-milled powders were subjected to a postannealing up to 950 °C for 1 h with 5 °C/min heating rate and 10 °C/min cooling rate. The SBT bulk sample was prepared by sintering the 30 h milled powder at 1225 °C for 2 h. Both the annealed powder and sintered bulk sample were characterized by x-ray diffraction (XRD, X'Pert, Philips). To study the temperature induced ferroelectric phase transition in SBT powder, *in situ* high temperature Raman experiments were carried out using a TMS 93 Linkam thermal stage capable of holding temperature over the range between 300 and 770 K. All micro-Raman spectra were measured in the backscattering geometry using a Jobin Yvon T64000 Raman spectrometer with an Olympus microscope attachment and equipped with a liquid-nitrogen-cooled charge coupled device (CCD) detector. The 514.5 nm line of an argon-ion laser was used as the excitation source.

III. RESULTS AND DISCUSSION

Figure 1 shows the XRD patterns of the samples annealed at various temperatures and the sintered bulk sample. The polycrystalline single phase SBT was formed in all annealed samples and this SBT phase was well established with

^{a)} Author to whom correspondence should be addressed; electronic mail: physzx@nus.edu.sg

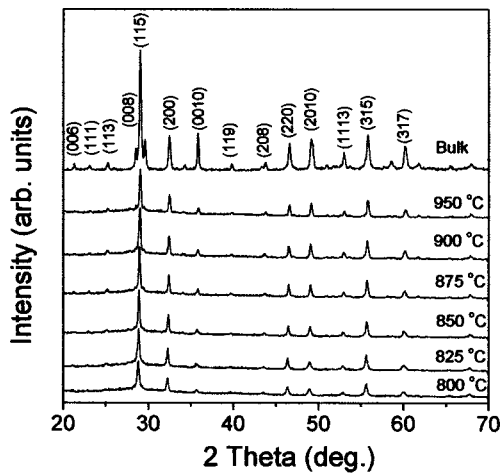


FIG. 1. XRD patterns of sintered bulk sample and samples annealed at various temperatures.

the increase of annealing temperatures.¹⁶ After fitting the XRD patterns with a Gaussian line shape, the average particle size was determined from the full width at half maximum (FWHM) of the strongest x-ray diffraction peak (115) using Scherrer equation which assumes the small crystallite size to be the only case of line broadening¹⁷

$$D_{XRD} = K\lambda / B \cos \theta, \quad (1)$$

where D_{XRD} is the particle diameter, λ is the x-ray wavelength, B is the FWHM of the diffraction line, θ is the angle of diffraction, and the constant $K \approx 1$. In order to remove the contribution from instrumental broadening, the FWHM of the (115) line in XRD trace of the sintered bulk sample was subtracted as described by Eq. (2)¹⁸

$$B^2 = a^2 - b^2, \quad (2)$$

where B is the FWHM of the true diffraction profile, a and b are the measured FWHM of equivalent diffraction lines in the annealed powders and the sintered bulk sample, respectively. The calculated size of our annealed SBT powders ranges from 11 to 71 nm.

Figure 2 shows the temperature dependence of the low-frequency (10–300 cm^{-1}) Raman spectra of the bulk sample. The lowest frequency peak, $A_1(z)$ mode shows an obvious redshift and broadening with increasing temperature, especially mostly softens near 560 K, and disappears above 580 K as shown in Fig. 2 inset. This typical soft mode behavior is responsible for the ferroelectric phase transition in bulk SBT sample.¹⁹ It is noted that the lowest frequency peak A_1 disappears below the Curie temperature ($T_c = 589$ K) obtained from the temperature dependence of dielectric constant (shown in Fig. 2 inset). A similar phenomenon has been reported by Kojima.^{19,20} Thus, the phase transition temperatures in SBT powders cannot be directly read from the *in situ* Raman spectra as previous Raman scattering studies in BaTiO_3 ,²¹ PbTiO_3 ,¹³ and $\text{PbZr}_{1-x}\text{Ti}_x\text{O}_3$.²²

Following Burns and Scott²³ and Kojima,^{19,20} we fitted the soft mode A_1 by a simple damped harmonic oscillator model after the correction of the Bose factor. According to the following two equations:

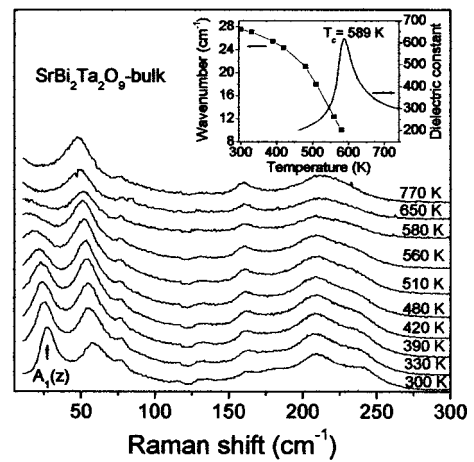


FIG. 2. Low-frequency Raman spectra of SBT bulk sample as a function of temperature. The inset shows the temperature dependencies of dielectric constant and frequency of soft mode of the SBT bulk sample.

$$\omega_p = \omega_{TO} \left[1 - \frac{1}{2} (\gamma / \omega_{TO})^2 \right]^{1/2}, \quad (3)$$

$$\frac{I(\omega_p)}{I(0)} = \frac{(\omega_{TO} / \gamma)^2}{1 - \frac{1}{4} (\gamma / \omega_{TO})^2} \quad (4)$$

we measured the frequency corresponding to the peak intensity, ω_p , the intensity at the peak, $I(\omega_p)$, and the intensity at zero frequency, $I(0)$. A computer fitting with a Lorentzian line shape was carried out and the damping factors γ were obtained. Figure 3 shows the damping factors of the soft mode $A_1(z)$ for the SBT bulk sample and nanoparticles as a function of temperature. The dark symbols represent the damping factors obtained from Eqs. (3) and (4). The solid lines are fitting results by the universal scaling theory which predicted the temperature dependence of damping factors $\gamma(T)$ of the soft modes as²⁴

$$\gamma(T) = \gamma(0) t^{-0.5}, \quad (5)$$

where $t = (T_c - T) / T_c$. The good agreements between the experimental data and the theoretical fitting results were ob-

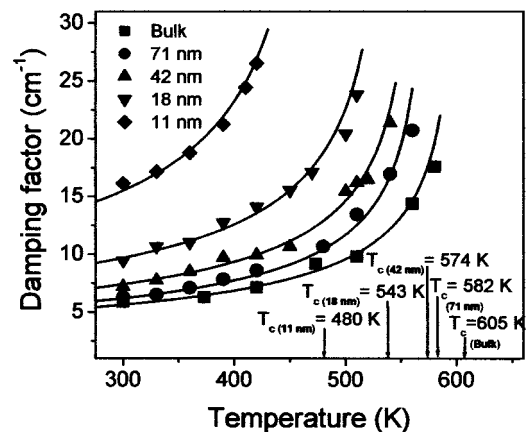


FIG. 3. Temperature dependence of damping factors of SBT bulk sample and nanoparticles of various sizes. The arrows indicate the transition temperature T_c .

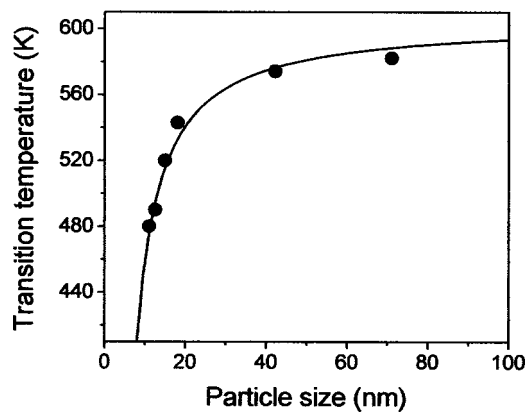


FIG. 4. Ferroelectric transition temperatures as a function of particle size.

served in both the bulk sample and nanoparticles with various particle sizes. The estimated ferroelectric phase transition temperatures were also indicated by the arrows in Fig. 3.

Figure 4 shows the phase transition temperatures T_c as a function of particle size. Similar to the previous study of size effects on PbTiO_3 nanoparticles,¹³ the transition temperatures of SBT ultrafine particles markedly decrease as particle size decreases, in particular when the particle size is less than 20 nm in this work. The solid line in Fig. 4 is the value obtained by the following equation:¹³

$$T_c(D) = T_c(\infty) - C/(D - D'), \quad (6)$$

where $T_c(D)$ is the transition temperature of the particles with D nm in size; $T_c(\infty)$ is the transition temperature of the bulk sample, which is taken to be 605 K (see Fig. 3) although it is relatively higher than T_c obtained from dielectric constant; T_c of SBT nanoparticles was derived from Raman scattering, C and D' are fitting parameters. The above equation was first proposed by Ishikawa, Yoshikawa, and Okada¹³ and the qualitative understanding based on the soft mode picture was given by Zhong *et al.*²⁵ According to previous definition,^{13,25} a critical size D_{crit} is the size at which $T_c = 0$ K. We obtained D_{crit} of SBT from Eq. (6) to be 2.6 nm. This value is much less than the values of PT, which is 13.8 nm derived by Raman scattering,¹³ 8.8 nm by specific heat measurement,²⁵ and 7 nm by x-ray diffraction.¹² It is even less than that of PZT (4 nm¹⁰ and 4.2 nm⁹). This small critical size indicates another potential application of SBT as a promising ferroelectric material for the formation of low dimension and high density ferroelectric device besides being fatigue free.

IV. CONCLUSION

The size effect on the ferroelectric phase transition in $\text{SrBi}_2\text{Ta}_2\text{O}_9$ nanoparticles has been studied by *in situ* Raman scattering. With the decrease of particle size, the transition temperature decreases dramatically. From an empirical expression, the critical size ($D_{\text{crit}} = 2.6$ nm) of SBT was obtained. Ferroelectricity will be lost when the particle size is less than D_{crit} . Compared with other ferroelectric materials, SBT has a relatively smaller critical size, which implies that SBT is a potential candidate for formation of ferroelectric devices of ultrafine size.

¹J. F. Scott and C. A. Araujo, *Science* **246**, 1400 (1989).

²O. Auciello, J. F. Scott, and R. Ramesh, *Phys. Today* **51**, 22 (1998).

³B. H. Park, B. S. Kang, S. D. Bu, T. W. Noh, J. Lee, and W. Jo, *Nature (London)* **401**, 682 (1999).

⁴C. A. P. de Araujo, J. D. Cuchiaro, L. D. McMillan, M. C. Scott, and J. F. Scott, *Nature (London)* **374**, 627 (1995).

⁵R. E. Newnham, R. W. Wolfe, R. S. Horsey, F. A. Diaz-Colon, and M. I. Kay, *Mater. Res. Bull.* **8**, 1183 (1973).

⁶A. D. Rae, J. G. Thompson, and R. L. Withers, *Acta Crystallogr., Sect. B: Struct. Sci.* **48**, 418 (1992).

⁷C. L. Wang, W. L. Zhong, and P. L. Zhang, *J. Phys.: Condens. Matter* **3**, 4743 (1992).

⁸H. K. Sy, *J. Phys.: Condens. Matter* **5**, 1213 (1993).

⁹W. L. Zhong, Y. G. Wang, P. L. Zhang, and B. D. Qu, *Phys. Rev. B* **50**, 698 (1994).

¹⁰H. T. Huang, C. Q. Sun, T. S. Zhang, and P. Hing, *Phys. Rev. B* **63**, 184112 (2001).

¹¹T. Yu, Z. X. Shen, J. M. Xue, and J. Wang, *J. Appl. Phys.* **93**, 3470 (2003).

¹²S. Chattopadhyay, P. Ayyub, V. R. Palkar, and M. Multani, *Phys. Rev. B* **52**, 13177 (1995).

¹³K. Ishikawa, K. Yoshikawa, and N. Okada, *Phys. Rev. B* **37**, 5852 (1988).

¹⁴M. H. Frey, Z. Xu, P. Han, and D. A. Payne, *Ferroelectrics* **206**, 337 (1998).

¹⁵X. S. Gao, J. M. Xue, J. Wang, T. Yu, and Z. X. Shen, *J. Am. Ceram. Soc.* **85**, 565 (2002).

¹⁶R. R. Das, W. Perez, R. S. Katiyar, and A. S. Bhalla, *J. Raman Spectrosc.* **33**, 219 (2002).

¹⁷A. J. C. Wilson, *Proc. Phys. Soc. London* **80**, 286 (1962).

¹⁸B. E. Warren, *X-Ray Diffraction* (Addison-Wesley, New York, 1969).

¹⁹S. Kojima, *J. Phys.: Condens. Matter* **10**, L327 (1998).

²⁰S. Kojima and I. Saitoh, *Physica B* **263–264**, 653 (1999).

²¹K. Uchino, E. Sadanaga, and T. Hirose, *J. Am. Ceram. Soc.* **72**, 1555 (1989).

²²A. G. Souza Filho, K. C. V. Lima, A. P. Ayala, I. Guedes, P. T. C. Freire, F. E. A. Melo, J. Mendes Filho, E. B. Araujo, and J. A. Eiras, *Phys. Rev. B* **66**, 1321071 (2002).

²³G. Burns and B. A. Scott, *Phys. Rev. B* **7**, 3088 (1973).

²⁴A. P. Levanyuk and N. V. Shchedrina, *Sov. Phys. Solid State* **16**, 923 (1974).

²⁵W. L. Zhong, B. Jiang, P. L. Zhang, J. M. Ma, H. M. Chen, Z. H. Yang, and L. Li, *J. Phys.: Condens. Matter* **5**, 2619 (1993).